

# Effects of Hafnium on Microstructure and Mechanical Properties in as-HIPed FGH4097 Powder Metallurgy Superalloy

ZHANG Yi-Wen<sup>1,2,a,\*</sup>, JIA Jian<sup>1,2</sup>, HAN Shou-Bo<sup>1,2</sup>, LIU Jian-Tao<sup>1,2</sup>

<sup>1</sup>High Temperature Material Institute, Central Iron and Steel Research Institute, Beijing 100081, China

<sup>2</sup>Beijing Key Laboratory of Advanced High Temperature Materials, Beijing 100081, China

<sup>a</sup>yiwen64@126.com

**Keywords:** PM Superalloy, FGH4097, Hafnium, PREP, Mechanical Properties

**Abstract.** New type powder metallurgy (PM) superalloy FGH4097 developed in China is applied in advanced aircraft engine hot section components such as turbine disc and compressor disc. FGH4097 alloy billets ( $\Phi 80 \times 135$ mm) in the study were processed via plasma rotating electrode processing (PREP) powder making, hot isostatic pressing (HIP) forming and heat treatment. Range of powder size is 50~150 $\mu$ m. HIP parameters are 1180~1220 $^{\circ}$ C, 130MPa and 4hrs. The heat treatment process of FGH4097 alloy billet is solution treatment plus three stages aging treatment. By means of metallurgical microscope, scanning electron microscope and physiochemical phase analysis, the influence of Hafnium with different contents on the grain size,  $\gamma'$  phase, MC carbide in as-HIPed FGH4097 alloy have been studied, also influences of Hafnium contents on mechanical properties including tensile properties, stress rupture properties and fatigue crack propagation rate have been investigated. The results showed that Hf had no effect on grain size,  $\gamma'$  phase size and MC carbide size and morphology. Hf promoted  $\gamma'$  phase and MC carbide precipitation, changed  $\gamma'$  phase and MC carbide chemical constitutions and accelerated the splitting of  $\gamma'$  phase to preferably stable cubic. Proper Hf content plays a beneficial role in improving the comprehensive mechanical properties of FGH4097 alloy, which helps improve mechanical properties, including impact ductility, tensile plasticity, stress rupture life, and fatigue crack propagation resistance, also helps decrease notch sensitivity. FGH4097 alloy with 0.30wt%Hf content presents the optimum comprehensive mechanical properties.

## 1. Introduction

Microelement Hf added in Ni-based powder metallurgy (PM) superalloy can modify microstructure and improve stress rupture life, creep resistance, crack propagation resistance and eliminate notch sensitivity<sup>[1-4]</sup>. Microelement Hf promotes the precipitation of  $\gamma'$  phase and MC carbide, which result in Hf contained  $\gamma'$  phases and MC carbide precipitation, and their constitution changing<sup>[5,6]</sup>. Usually Hf is added to the composition of the advanced PM superalloys to change the mechanism of the MC carbide precipitation from the boundaries of grains and particles to inside the grains.

Previous research shown that Hf changed the morphology of  $\gamma'$  phase in Ni-based PM superalloy. For example, Hf improved  $\gamma'$  phase growth in IN100 PM alloy, cubic  $\gamma'$  phase size in alloy contained 1.05%Hf (mass fraction; without notification, the following Hf content unit is mass fraction) was bigger than that contained 0.40%Hf, while Hf showed no apparent strengthening effect in alloys<sup>[1]</sup>. The addition of Hf in NASA IIB-11 PM alloy could improve latticed  $\gamma'$  phase precipitation<sup>[5]</sup>. It is reported that adding 0.25-1.7%Hf in Astroloy PM alloy



influenced morphology of  $\gamma'$  phase apparently<sup>[6]</sup>. With Hf content increasing, the  $\gamma'$  phase arranges fan shape, which could be explained as one or more  $\gamma'$  phases nucleated at grain boundary and grew in matrix. At the same time some elements diffused from matrix into  $\gamma'$  phases to promote formation of  $\gamma'$  phase branching, then  $\gamma'$  phase grows radically and arranges fan shape<sup>[6]</sup>. With appropriate Hf content addition in Ni-based PM superalloy, MC carbide precipitation distributed dispersally<sup>[1,2,6]</sup>. Under the action of elastic strain field, the cubic  $\gamma'$  phase splitted into other morphology, like doublet of plates or octet of cubes. And the size of  $\gamma'$  phase will be smaller<sup>[7-10]</sup>. In summary, the morphology of  $\gamma'$  phase will be different in different PM superalloy with Hf content.

IN100 alloy with 0.4% Hf content (MERL76 alloy) prepared by argon atomization and hot isostatic pressing (HIP) showed that the stress rupture life of MERL76 alloy was ten times longer than that of IN100 alloy at the condition of 732 °C and 655 MPa. The stress rupture ductility was much better and there was no notch sensitivity in MERL76 alloy<sup>[1]</sup>. EP741 alloy with 0.3% Hf content (EP741NP alloy) prepared by plasma rotating electrode process (PREP) atomization and HIP showed that both stress rupture life and ductility at 750 °C were improved<sup>[2-4]</sup>. Because Hf forms primary MC carbides that remain stable at low temperatures, which is considered to prevent excessive  $M_{23}C_6$  and  $M_6C$  formation at grain boundaries, RR1000 alloy<sup>[11,12]</sup> (0.75% Hf), N18 alloy<sup>[12,13]</sup> (0.5% Hf) and N19 alloy<sup>[14]</sup> (0.25% Hf) showed improved creep resistance and crack propagation resistance.

The addition of too much Hf has little effect on improving mechanical properties of Ni-based PM superalloy<sup>[2]</sup>. Till now the content of Hf is lower than 0.8% in N18, RR1000 and EP741NP alloys<sup>[4,12,15]</sup>. Investigations about the effect of Hf addition on mechanical properties in PM superalloys have not been addressed systematically in literatures. Thus, this paper investigated the effects of Hf contents (0, 0.16, 0.30, 0.58 and 0.89%) on chemical constitution, morphology, size and volume fraction of  $\gamma'$  phase and MC carbide. The effects of Hf contents on impact ductility, tensile properties (at room temperature, 650 °C and 750 °C), stress rupture properties (at 650 °C) and fatigue crack growth rate (at 650 °C) have also been studied. According to the results, the reasonable Hf content was given. This work is helpful to understand Hf effects on mechanical properties in PM superalloy and to design Ni-based PM superalloy with high strength as well as high damage tolerance.

## 1 Materials and methods

The experimental material was Ni-based PM superalloy FGH4097 with different Hf contents. The chemical composition (mass fraction, %) of FGH4097 is: Co16.0, (Cr+W+Mo) =18.5, (Al+Ti+Nb)=9.4, Hf 0-0.89, C minor, B minor, Zr minor, and Ni balance. The contents of Hf (mass fraction, %) were 0, 0.16, 0.30, 0.58 and 0.89. Powders (50-150  $\mu\text{m}$ ) prepared by PREP and HIPed at 1200 °C. HIP billets heat treatment process was 1200 °C/4 h/AC + three stages aging treatment. The last aging treatment was 700 °C/(15-20)h/AC.

The chemical constitution and contents of  $\gamma'$  phase and MC carbide phase have been analyzed by physiochemical phase analysis. Carbide morphology has been observed by JSM-6480L scanning electron microscope (SEM), size of carbide has been analyzed by image analyzer (ten times at 500x). Microstructure of  $\gamma'$  phase has been observed by JSM-6480L SEM and SUPRA 55 FEG-SEM. SEM samples for microstructure observation were prepared by electrolytic polishing and electrolytic erosion. The electrolytic polishing was carried out in 20%  $\text{H}_2\text{SO}_4$ +80%  $\text{CH}_3\text{OH}$  solution, at 30V and 15-20s, the electrolytic polishing erosion was carried out in 85ml  $\text{H}_3\text{PO}_4$ +5ml  $\text{H}_2\text{SO}_4$ +8g  $\text{CrO}_3$  solution, at 5V and 3~6s respectively. Size of  $\gamma'$  phase has been analyzed by Image-Pro Plus 6.0 software. The impact ductility, tensile

properties(at room temperature, 650°C and 750°C) have been tested. Stress rupture life at 650°C /1020MPa has been tested at smooth and notched samples(radius of notch R=0.15mm). The fatigue crack growth rate at 650°C has been tested under condition of stress ratio R=0.05 and load frequency 10-30 cycle/min. The samples were prepared by mechanical polishing and chemical etching (etched by 3gCuSO<sub>4</sub>+80mlHCl+40ml C<sub>2</sub>H<sub>5</sub>OH solution). After chemical etching,  $\gamma'$  phase is etched away and  $\gamma$ -matrix is left behind, then these samples have been used to micro-hardness test in MTS XP Nano Indenter(three points in one sample). The effect of Hf content on micro-hardness of  $\gamma$ -matrix in FGH4097 alloy has been investigated.

## 2. Experimental results

### 2.1 Phases in FGH4097 alloy

The experimental results showed that FGH4097 alloy consists of  $\gamma$  matrix,  $\gamma'$  phase, MC carbide, small amounts of M<sub>6</sub>C carbide and M<sub>3</sub>B<sub>2</sub> boride, and  $\gamma'$  phase and MC carbide are the main precipitates. The results of physicochemical phase analysis of the phase content in FGH4097 alloy with different Hf contents was given in Table 1. With the increase of Hf content, the amount of MC carbide increases and the amount of  $\gamma'$  phase also increases slightly. The amount of  $\gamma'$  phase is about 62%, the amount of MC carbide is no more than 0.34%, and the total amount of M<sub>6</sub>C carbide and M<sub>3</sub>B<sub>2</sub> is no more than 0.21%. Thus, no new phase was found in FGH4097 alloy with different Hf contents. The grain shapes were regular, the grain sizes were 30 ~ 40 $\mu$ m which keeps in a stable level in FGH4097 alloy when Hf contents changed from 0 to 0.89%.

Table 1 The amount of phases in FGH4097 alloy with different Hf contents (mass fraction, %)

Hf content	$\gamma$	$\gamma'$	MC	M <sub>6</sub> C+M <sub>3</sub> B <sub>2</sub>
0	37.678	61.930	0.264	0.128
0.16	37.503	62.080	0.266	0.151
0.30	37.378	62.180	0.270	0.172
0.58	37.062	62.450	0.293	0.195
0.89	36.762	62.690	0.338	0.210

### 2.2 Morphology and chemical constitution of $\gamma'$ phase

In FGH4097 alloy with five Hf contents,  $\gamma'$  phase distributed in grains and at grain boundaries. There are three kinds of  $\gamma'$  phase: the large  $\gamma'$  phase precipitated from  $\gamma$  solid solution during solution cooling which is called primary  $\gamma'$  phase at grain boundaries, square  $\gamma'$  phase precipitated in grains precipitated from  $\gamma$  solid solution during solution cooling which is called secondary  $\gamma'$  phase, fine and square  $\gamma'$  phase precipitated in grains from  $\gamma$  solid solution during aging which is called ternary  $\gamma'$  phase. Figure 1 showed the morphology of  $\gamma'$  phase in FGH4097 alloy with 0.30% Hf content,  $\gamma'$  phase at grain boundaries and secondary  $\gamma'$  phase are block shapes (Fig.1a) and ternary  $\gamma'$  showed spherical particles (Fig.1b).

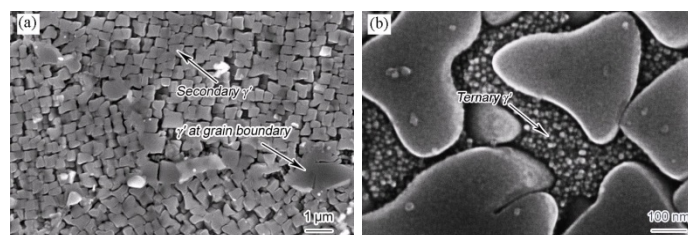


Fig.1 Low (a) and high (b) magnified SEM images of  $\gamma'$  phase in FGH4097 alloy with 0.30% Hf

The experimental results showed that the addition of small amount of Hf in FGH4097 alloy does not change morphology of  $\gamma'$  phase at grain boundaries and ternary  $\gamma'$  phases, but greatly influence morphology of secondary  $\gamma'$  phase. Figure 2 showed SEM images of secondary  $\gamma'$  phase in FGH4097 alloy with different Hf contents. The secondary  $\gamma'$  phase is mainly cubic in the alloys without Hf and with 0.16wt% Hf contents (Fig. 2a, b). As the amount of Hf increases, the secondary  $\gamma'$  phase grows and splits. For FGH4097 alloy with 0.30% Hf content, the secondary  $\gamma'$  phase is mainly octahedron cubic and butterfly-like shape (Fig. 2c). For FGH4097 alloy with 0.58% Hf content, the secondary  $\gamma'$  phase is mainly cubic and octahedron cubic (Fig. 2d). The secondary  $\gamma'$  phase is mainly cubic in the alloy with 0.89% Hf content (Fig. 2e).

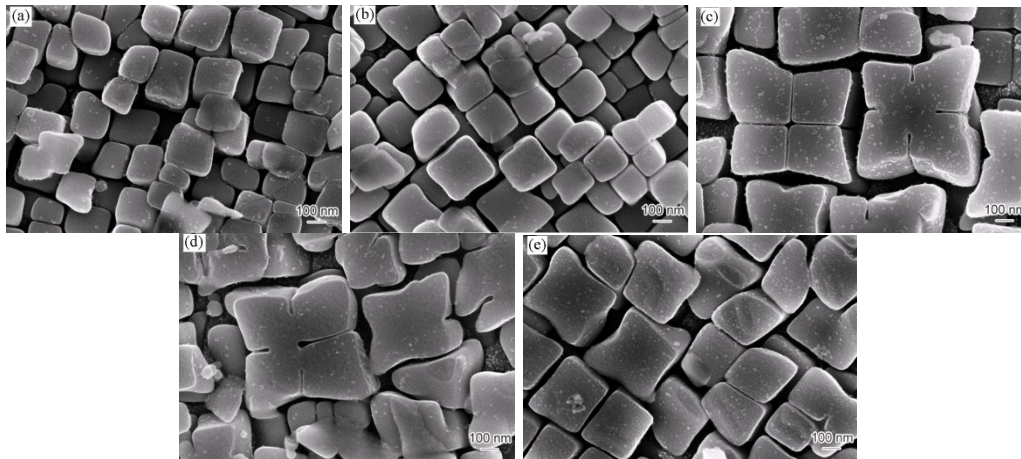
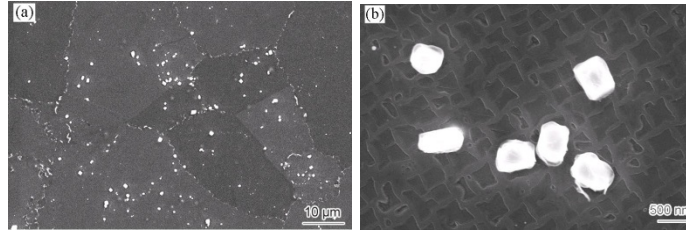


Fig.2 SEM images of secondary  $\gamma'$  phase in FGH4097 alloys with 0 (a), 0.16% (b), 0.30% (c), 0.58% (d) and 0.89% (e) Hf respectively

When Hf element was added into FGH4097 alloy, because of Hf replacing Al, the chemical constitution of  $\gamma'$  phase is  $(\text{Ni},\text{Co})_3(\text{Al},\text{Ti},\text{Nb},\text{Hf})$  which contain Ni, Co, Al, Ti, Nb and Hf. With the increase of Hf content in the alloy, Hf content in  $\gamma'$  phase increases gradually, while Al content decreases gradually, and more amount Al replaced by Hf. When Hf content is 0, 0.16, 0.30, 0.58 and 0.89%, chemical constitution of  $\gamma'$  phase are  $(\text{Ni}_{0.852}\text{Co}_{0.148})_3(\text{Al}_{0.783}\text{Ti}_{0.129}\text{Nb}_{0.088})$ ,  $(\text{Ni}_{0.854}\text{Co}_{0.146})_3(\text{Al}_{0.781}\text{Ti}_{0.129}\text{Nb}_{0.088}\text{Hf}_{0.002})$ ,  $(\text{Ni}_{0.855}\text{Co}_{0.145})_3(\text{Al}_{0.778}\text{Ti}_{0.129}\text{Nb}_{0.088}\text{Hf}_{0.005})$ ,  $(\text{Ni}_{0.856}\text{Co}_{0.144})_3(\text{Al}_{0.773}\text{Ti}_{0.129}\text{Nb}_{0.088}\text{Hf}_{0.010})$  and  $(\text{Ni}_{0.857}\text{Co}_{0.143})_3(\text{Al}_{0.767}\text{Ti}_{0.129}\text{Nb}_{0.088}\text{Hf}_{0.016})$ , respectively. With the increase of Hf content in the alloy, size of ternary  $\gamma'$  phase keeps in a stable level and average size is 14-18nm. Sizes of  $\gamma'$  phase at grain boundaries and secondary  $\gamma'$  phase increase firstly and then decrease gradually. Average size of  $\gamma'$  phase at grain boundary is 820-1450nm and that of secondary  $\gamma'$  phase is 276-511nm. Sizes of  $\gamma'$  phase at grain boundaries and secondary  $\gamma'$  phase in 0.30% Hf content FGH4097 alloy have the maximum size values which are average 1450nm and 551nm, respectively. Size of secondary  $\gamma'$  phase in FGH4097 alloy with different Hf contents showed a normal distribution.

### 2.3 Morphology and chemical constitution of MC carbide

Addition of Hf in FGH4097 alloy did not change the morphology of MC carbide. Granular MC carbide distributed in grains and at grain boundaries, MC carbide precipitated at grain boundaries has larger size. With the increase of Hf content in FGH4097 alloy, Size of MC carbide keeps in a stable level and the average size is  $0.878\sim 1.064\mu\text{m}$ . Figure 3 showed SEM images of MC carbide in FGH4097 alloy with 0.30% Hf content.



*Fig.3 Low (a) and high (b) magnified SEM images of MC carbide of FGH4097 alloy with 0.30% Hf*

When Hf is added in FGH4097 alloy, MC carbide chemical constitution is (Nb, Ti, Hf)C, which mainly contained Nb, Ti, Hf and C. When the content of Hf is 0, 0.16, 0.30, 0.58% and 0.89%, chemical constitutions of MC carbide are (Nb<sub>0.664</sub>Ti<sub>0.336</sub>)C, (Nb<sub>0.654</sub>Ti<sub>0.323</sub>Hf<sub>0.023</sub>)C, (Nb<sub>0.642</sub>Ti<sub>0.308</sub>Hf<sub>0.050</sub>)C, (Nb<sub>0.619</sub>Ti<sub>0.280</sub>Hf<sub>0.101</sub>)C and (Nb<sub>0.574</sub>Ti<sub>0.253</sub>Hf<sub>0.173</sub>)C, respectively.

## 2.4 Mechanical properties

### 2.4.1 Impact toughness

The experimental results showed that addition of Hf apparently influences impact toughness at room temperature. Figure 4 showed the impact energy absorption at room temperature in FGH4097 alloy with different Hf contents. With the increase of Hf content, impact absorption increased at first and then decreased. Impact energy absorption value of the alloy with 0.16% Hf content is the highest, that of the alloy with 0.30wt% Hf content is the second highest one and that of the alloy with 0.89% Hf content is the lowest one. Compared with 0.30% Hf content, impact energy absorption values of the alloys without Hf and with 0.89% Hf content alloy were reduced by 11.2% and 21.0% respectively, the impact toughness decreased obviously.

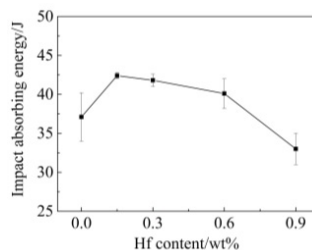


*Fig.4 Impact absorbing energy of FGH4097 alloy with different Hf contents at room temperature*

### 2.4.2 Tensile properties

Tensile properties of FGH4097 alloy with different Hf contents at room temperature has been shown in Fig.5. Hf content has little effect on the tensile strength and yield strength at room temperature. Room temperature tensile strength of 0.16% Hf content FGH4097 alloy is slightly higher, and 0.30% Hf content FGH4097 alloy has the lowest tensile strength at room temperature. Tensile ductility changes with the increase of Hf content. Tensile ductility of 0.16% Hf content FGH4097 alloy is the lowest, while tensile ductility is the highest when Hf content is 0.30%.

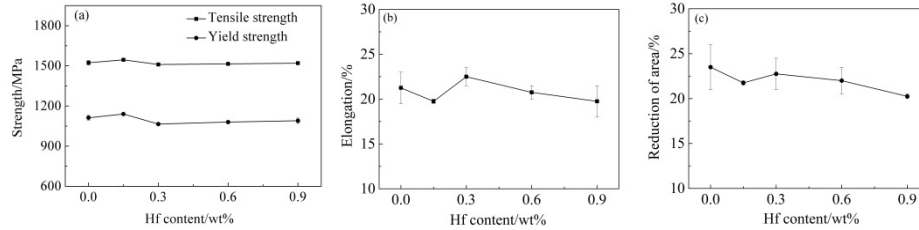


*Fig.5 Strength (a), elongation (b), reduction of cross sectional area (c) of FGH4097 alloy with different Hf content at room temperature*

Tensile test of FGH4097 alloy with different Hf contents at 650°C has been shown in Fig.6. with Hf content increasing, curves of tensile strength changing at 650°C is similar to those at the room temperature. Hf content has little effect on tensile strength and yield strength, but influence tensile ductility to some degree. When Hf content is 0.30%, tensile strength is the lowest and ductility is the highest. When Hf content is 0.16%, tensile strength is the highest and ductility is the lowest.

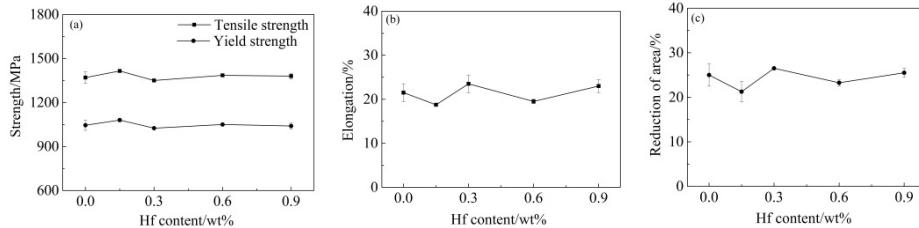


*Fig.6 Strength (a), elongation (b), reduction of cross sectional area (c) of FGH4097 alloy with different Hf content at 650 °C*

Influence of Hf content on tensile properties of FGH4097 alloy at 750°C is the same as that at 650°C. Tensile properties with different Hf contents in FGH4097 alloy at 750°C is shown in Fig.7. Hf content has little effect on tensile strength and yield strength, while has more effect on the tensile plasticity. When Hf content is 0.30%, tensile strength is the lowest and ductility is the highest. When Hf content is 0.16%, tensile strength is the highest and ductility is the lowest.

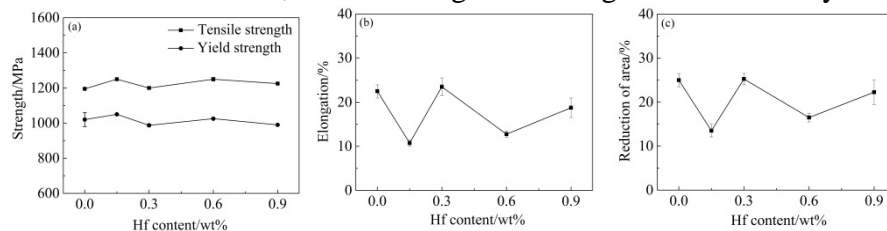


*Fig.7 Strength (a), elongation (b), reduction of area (c) of FGH4097 alloy with different Hf contents at 750 °C*

### 2.4.3 Stress rupture properties at high temperature

Under 650°C/1020MPa test condition, stress rupture life of smooth sample and notch sample (R=0.15mm) in FGH4097 alloy with different Hf contents were shown in Figure 8. Stress rupture life of notch specimens increased with Hf content increasing. Stress rupture life of notch specimen with 0.30% Hf content is the longest one. Stress rupture life of notch specimen with no Hf content is shorter than that of smooth specimen and notch sensitivity exists. When Hf content is higher than 0.16%, stress rupture life of notch specimen is longer than that of smooth specimen and notch sensitivity does not exist. The law of rupture ductility with Hf content

changing is the same as the tensile ductility in FGH4097 alloy, rupture ductility of the alloy with 0.30% Hf content is the highest value.

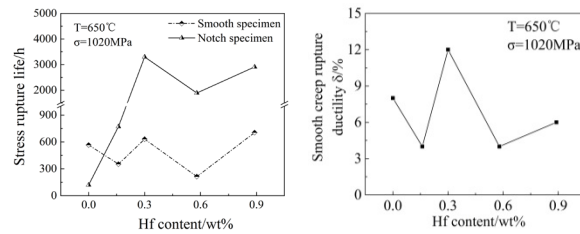


Fig.8 Stress rupture life of FGH4097 alloy with different Hf contents at 650 °C/1020MPa

#### 2.4.4 Fatigue crack propagation rate

Figure 9 showed the relationship between fatigue crack propagation rate ( $da/dN$ ) and stress intensity factor range ( $\Delta K$ ) in FGH4097 alloy with different Hf contents under condition of 650 °C/R=0.05/0.33Hz. The  $da/dN$  of FGH4097 alloy with 0.30% Hf content is the lowest during the  $\Delta K$  range of 28.5~33.2 MPa $\cdot$ m<sup>1/2</sup>. When  $\Delta K=30$ MPa $\cdot$ m<sup>1/2</sup>, the fatigue crack propagation rate values of the alloys with 0, 0.16, 0.30, 0.58 and 0.89% Hf content are  $2.50\times 10^{-3}$ ,  $1.47\times 10^{-3}$ ,  $4.85\times 10^{-4}$ ,  $1.04\times 10^{-3}$  and  $1.04\times 10^{-3}$  mm/cycle, respectively. The  $da/dN$  value of the alloy with 0.30% Hf content is one-fifth of that of the alloy without Hf content.

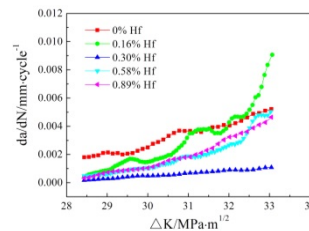


Fig.9 Fatigue crack propagation rate of FGH4097 alloy with different Hf contents at 650 °C

### 3. Discussions

It can obviously improve the ductility when small amount of Hf is added in FGH4097 alloy. Especially, mechanical properties are obviously improved when Hf content is 0.30%. Hf addition changes distribution of alloy elements between phases and affects microstructure and properties. Notch sensitivity elimination is strongly dependent on ductility of  $\gamma$  matrix solid solution. Hf is a strong carbide-forming element. Hf partitions to MC carbide firstly and then to  $\gamma'$  phase. Hf modifies the chemical constitutions of MC phase,  $\gamma'$  phase and  $\gamma$  matrix, which led to redistribution of elements Ti, Nb, W, Mo, and Cr in MC,  $\gamma'$  phase and  $\gamma$  matrix.

When Hf is 0.3% content, Hf can effectively replace Nb and Ti in MC. The displaced Nb and Ti partition to  $\gamma$  matrix and form NbC and TiC respectively in  $\gamma$  matrix. As a result, C content in  $\gamma$  matrix decreases which decreases  $\gamma$  matrix strength and improves ductility of the alloy. Particularly, although the tensile strength decreased slightly, the strength matched well with ductility. It can also decrease crack propagation rate, improve impact toughness, eliminate notch sensitivity of stress rupture. If Hf content is not enough, Hf can not effectively replace Nb and Ti in MC, the strength of  $\gamma$  matrix will not decrease efficiently. If Hf content is too much, Hf will form HfC or HfO<sub>2</sub> and hardly replaces Nb and Ti in MC. The results by MTS Nano Indenter XP showed that the hardness of  $\gamma$  matrix in alloy with 0.30% Hf content is the lowest which means  $\gamma$  matrix strength is the lowest. Thus, the amount of Hf in FGH4097 alloy should be added properly.

#### 4. Conclusions

(1) Precipitation phases of FGH4097 alloy with different Hf content are mainly  $\gamma'$  phase, MC carbide and small amount of  $M_6C$  carbide as well as  $M_3B_2$  boride. When Hf is added in FGH4097 alloy, part of Hf replace Al atoms in  $\gamma'$  phase, constitution of  $\gamma'$  phase is  $(Ni,Co)_3(Al,Ti,Nb,Hf)$ ; part of Hf replace Ti and Nb atoms in MC type carbide, constitution of MC carbide is  $(Nb,Ti,Hf)C$ . As Hf contents increasing,  $\gamma'$  phase fraction slightly increased and MC carbide fraction increases apparently. Hf addition in FGH4097 alloy does not influence size and morphology of MC carbide, but significantly affects size and morphology of  $\gamma'$  phase. Hf enters into  $\gamma'$  phase and changes the elastic interaction energy distribution of  $\gamma'$  phase during growth, which accelerate cubic  $\gamma'$  phase splitting into 8 small cubic and promote  $\gamma'$  phase forming stable cubic state preferably. Since the addition of Hf effects the distribution of alloy elements between phases, thereby improving the ductility of the  $\gamma$  matrix solid solution with the optimal Hf, which is beneficial for reducing the notch sensitivity.

(2) Hf content does not influence tensile strength of FGH4097 alloy significantly, but influence its impact toughness and tensile ductility obviously. Under 650°C/1020MPa condition, stress rupture life of notch sample is shorter than that of smooth one when there is no Hf addition. Hf addition decreases the notch sensitivity of sample, proper Hf addition can improve the fatigue crack propagation resistance.

(3) The best comprehensively mechanical properties including tensile strength, stress rupture property, plasticity, toughness and crack propagation resistance can be reached in 0.30% Hf content FGH4097 alloy.

(4) Proper Hf addition in FGH4097 alloy can effectively change redistribution of elements between precipitation and  $\gamma$  solid solution which means that the strength and ductility can have a good match. It can also decrease notch sensitivity of high temperature stress rupture and crack propagation rate.

(5) To significantly explain the mechanism of effect of Hf on the mechanical properties in FGH4097 alloy, more in-depth research and analysis are needed.

#### Acknowledgements

The authors would like to thank the financial support by International Science & Technology Cooperation Program of China (No 2014DFR50330).

#### References

- [1] Evans D J, Eng R D. Development of a high strength hot isostatically pressed(HIP) disk alloy, MERL76, Hausner H H, Antes H W, Smith G D. Modern Developments in Powder Metallurgy. Washington: MPIF and APMI. 1982, Vol. 14, 51-63.
- [2] Belov A F, Anoshkin N F, Fatkullin O Kh, et al. Features of alloying of high-temperature alloys obtained by the metallurgical method of granules, Bannikh O A. Heat-resistant and Zharostoye Steels and Alloys on the Nickel Base. Moscow: Science, 1984, pp. 31-40.
- [3] Radavich J, Carneiro T, Furrer D, et al. Effect of processing and composition on the structure and properties of P/M EP741NP type alloys, Chinese Journal of Aeronautics, 20 (2007) 97-106. [https://doi.org/10.1016/S1000-9361\(07\)60013-2](https://doi.org/10.1016/S1000-9361(07)60013-2)
- [4] Radavich J, Furrer D, Carneiro T, et al. The microstructure and mechanical properties of EP741NP powder metallurgy disc material, Reed R C, Green K A, Caron P, et al(Eds.), Superalloys 2008, TMS, Pennsylvania, 2008, pp. 63-72.

- [5] Miner R V. Effects of C and Hf concentration on phase relations and microstructure of a wrought powder-metallurgy superalloy, *Metallurgical Transactions A*, 8 (1977) 259-263. <https://doi.org/10.1007/BF02661638>
- [6] Larson J M, Volin T E, Larson F G. In: Braun J D, Arrowsmith H W, McCall J L. *Microstructural Science*, American Elsevier Pub, New York, 1977, pp. 209-217.
- [7] Wang Y, Chen L Q, Khachaturyan A G. Kinetics of strain-induced morphological transformation in cubic alloys with a miscibility gap, *Acta Metallurgica et Materialia*, 41 (1993) 279-296. [https://doi.org/10.1016/0956-7151\(93\)90359-Z](https://doi.org/10.1016/0956-7151(93)90359-Z)
- [8] Qiu Y Y. Retarded coarsening phenomenon of  $\gamma'$  particles in Ni-based alloy. *Acta Materialia*, 44 (1996) 4969-4980. [https://doi.org/10.1016/S1359-6454\(96\)00128-0](https://doi.org/10.1016/S1359-6454(96)00128-0)
- [9] Yoo Y S, Yoon D Y and Henry M F. The effect of elastic misfit strain on the morphological evolution of  $\gamma'$ - precipitates in a model Ni-base superalloy, *Metals and Materials*, 1 (1995) 47-61.
- [10] Qiu Y Y. The splitting behavior of  $\gamma'$  particles in Ni-based alloys, *Journal of Alloys and Compounds*, 270 (1998) 145-153. [https://doi.org/10.1016/S0925-8388\(98\)00462-9](https://doi.org/10.1016/S0925-8388(98)00462-9)
- [11] Hardy M C, Zirbel B, Shen G. Developing damage tolerance and creep resistance in a high strength nickel alloy for disc applications, Green K A, Pollock T M, Haradra H, et al (Eds.), *Superalloys 2004*, TMS, Pennsylvania, 2004, pp. 83-90.
- [12] Starink M J, Reed P A S. Thermal activation of fatigue crack growth: Analysing the mechanisms of fatigue crack propagation in superalloys, *Materials Science and Engineering A*, 491 (2008) 279-289. <https://doi.org/10.1016/j.msea.2008.02.016>
- [13] Wlodek S T, Kelly M, Alden D. The structure of N18. Antolovich S D, Stusrud R W, Mackay R A, et al(Eds.), *Superalloys 1992*, TMS, Pennsylvania, 1992, pp. 467-476.
- [14] Guédou J-Y, Augustins-Lecallier I, Nazé L, et al. Development of a new fatigue and creep resistant PM nickel-base superalloy for disk applications. Reed R C, Green K A, Caron P, et al (Eds.), *Superalloys 2008*, TMS, Pennsylvania, 2008, pp. 21-30.
- [15] Flageolet B, Villechaise P, Jouiad M, Mendez J. Ageing characterization of the powder metallurgy superalloy N18. Green K A, Pollock T M, Haradra H (Eds.), *Superalloys 2004*, TMS, Pennsylvania, 2004, pp. 371-379.